Effects of Exceptional Points in PT-Symmetric Waveguides

Nimrod Moiseyev and Alexei A. Mailybaev

Abstract We start with a general theoretical introduction to $\mathscr{P}\mathscr{T}$-symmetric systems. Quantum systems with gain and loss can be modeled by non-Hermitian Hamiltonians, and $\mathscr{P}\mathscr{T}$-symmetry is a property that can be achieved, e.g. by a coupling with the laser field. The resulting $\mathscr{P}\mathscr{T}$-symmetric Hamiltonians possess a real spectrum (when the gain and loss are not too strong) and can be considered as a special case of pseudo-Hermitian Hamiltonians. The transition from a real to a complex spectrum occurs at the exceptional point (EP), where two eigenmodes coalesce both in eigenvalue and eigenvector. The $\mathscr{P}\mathscr{T}$-symmetric Hamiltonian can be realized experimentally in a system of two coupled waveguides with loss and gain. We describe in detail two physical effects related to the EPs in such a system. First, we show that light oscillations between two waveguides are suppressed by approaching the EP condition. Second, we prove that the group velocity of a light pulse decreases to zero as the system is tuned to be at the EP.

1 Introduction

Recently there has been an explosion of interest to $\mathscr{P}\mathscr{T}$-symmetric properties of non-Hermitian Hamiltonians, as first introduced by Bender and Boettcher [6]; see also [5, 14] and references therein. This symmetry is achieved when the parity transformation, $\mathscr{P}$, interchanges the system elements experiencing gain and loss, such that the system returns to its original form after the subsequent time reversal, $\mathscr{T}$. Under certain conditions $\mathscr{P}\mathscr{T}$-symmetric Hamiltonians can have a completely real

N. Moiseyev (✉)
Schulich Faculty of Chemistry and Faculty of Physics, Technion – Israel Institute of Technology, Haifa, Israel
e-mail: nimrod@technion.ac.il

A. A. Mailybaev
Instituto Nacional de Matemática Pura e Aplicada – IMPA, Rio de Janeiro, Brazil
e-mail: alexei@impa.br

D. Christodoulides, J. Yang (eds.), *Parity-time Symmetry and Its Applications*, Springer Tracts in Modern Physics 280,
https://doi.org/10.1007/978-981-13-1247-2_9

spectrum and, thus, can serve, under the appropriate inner product, as Hamiltonians of unitary quantum systems [28]. We should stress that although we focus on $\mathscr{P}\mathscr{T}$-symmetric systems, $\mathscr{P}\mathscr{T}$ symmetry is neither a necessary nor a sufficient condition for a non-Hermitian Hamiltonian to have a real spectrum [27, 28].

Why are the $\mathscr{P}\mathscr{T}$ properties of non-Hermitian Hamiltonians relevant to realistic physical systems? The realization of $\mathscr{P}\mathscr{T}$-symmetric "Hamiltonians" has been studied most recently for optical waveguides with complex refractive indices [13, 21, 22, 30]. The equivalence of the Maxwell and Schrödinger equations in certain regimes provides a physical system in which the properties of $\mathscr{P}\mathscr{T}$-symmetric operators can be studied and exemplified. In this chapter we will focus on the special effects of exceptional points (EPs) on the dynamical properties of $\mathscr{P}\mathscr{T}$-symmetric waveguides with complex index of refraction. The EP is a special type of a non-Hermitian degeneracy between two (or more) eigenstates formed by the coalescence of both eigenvalues and eigenvectors.

Quantum mechanics deals with matter waves and the effects of EPs in atomic and molecular systems have not been observed until now in experiments. Consider two atomic or molecular resonances, which are coupled by a CW-laser field (i.e., AC-electromagnetic field) to have the structure of the non-Hermitian Hamiltonian

$$\hat{H}_{NH} = \begin{pmatrix} E_1^{res} + \hbar\omega_L & d \\ d & E_2^{res} \end{pmatrix}, \tag{1}$$

where E_1^{res} and E_2^{res} are two complex autoionization or predissociation decay resonances; ω_L is fundamental frequency of the laser field; the off-diagonal elements d are proportional to the maximum amplitude of the laser field and describe the dipole transitions between the two metastable states. The imaginary parts of the complex eigenvalues E_1^{res} and E_2^{res} determine the decay rates, which are inversely proportional to the lifetimes of the corresponding metastable states [25]. In a special case, when the laser frequency is at the exact resonance

$$\hbar\omega_L = \mathrm{Re}\left(E_2^{res} - E_1^{res}\right), \tag{2}$$

a simple rewrite of the Hamiltonian (1) brings it to the form

$$\hat{H}_{NH} = \hat{H}_{\mathscr{P}\mathscr{T}} - i\frac{\Gamma_0}{2}\hat{I}, \tag{3}$$

where $\hat{I}$ is a identity operator and

$$\hat{H}_{\mathscr{P}\mathscr{T}} = \begin{pmatrix} E_0 + i\Gamma/2 & d \\ d & E_0 - i\Gamma/2 \end{pmatrix} \tag{4}$$

with $E_0 = \mathrm{Re}\, E_2^{res}$, $\Gamma = \mathrm{Im}\left(E_1^{res} - E_2^{res}\right)$ and $\Gamma_0 = -\mathrm{Im}\left(E_1^{res} + E_2^{res}\right)$. Here Γ_0 features the mean decay rate of both states. Due to Eq. (2), the diagonal elements

of $\hat{H}_{\mathscr{P}\mathscr{T}}$ have equal real parts and opposite imaginary parts. In this case the contribution $\hat{H}_{\mathscr{P}\mathscr{T}}$ to the full non-Hermitian Hamiltonian (3) is $\mathscr{P}\mathscr{T}$-symmetric; see Sect. 2 below. This observation provides a constructive way to design the $\mathscr{P}\mathscr{T}$ symmetry and EPs in realistic quantum systems.

In Sect. 2, we discuss basic features of $\mathscr{P}\mathscr{T}$-symmetric and pseudo-Hermitian Hamiltonians. These Hamiltonians possess real spectrum for the interval of parameters bounded by the EPs described in Sect. 3. Section 4 studies light propagation in a $\mathscr{P}\mathscr{T}$-symmetric system of coupled waveguides. Section 5 investigates the propagation of light pulses in the same system showing that light stops (the group velocity vanishes) exactly at the EP.

2 $\mathscr{P}\mathscr{T}$ Symmetry and Pseudo-Hermitian Hamiltonians

A quantum system is described by a Hermitian Hamiltonian $\hat{H}_0$. In the absence of magnetic field, this Hamiltonian is real and symmetric. Evolution of open quantum systems, when particles can be injected into or removed from the system, can be modeled by introducing a non-Hermitian part into the Hamiltonian, which describes the respective gain and loss. This non-Hermitian Hamiltonian part is given by $i\hat{V}$, where $\hat{V}$ is a real symmetric operator and i is the imaginary unit. In general, the resulting non-Hermitian Hamiltonian $\hat{H} = \hat{H}_0 + i\hat{V}$ has complex eigenvalues, $E = E_0 - i\Gamma/2$, where the real part is the energy and the imaginary part describes the rate of decay ($\Gamma > 0$) or growth ($\Gamma < 0$) of the respective metastable quantum state.

The spectrum of a non-Hermitian Hamiltonian may become real in a robust way when the system possesses an extra symmetry that accurately balances the gain and loss [6, 7, 21]. This can be understood using the example of a two-level system, where the first state $|1\rangle$ has energy E_0 and experiences gain, while the second state $|2\rangle$ has the same energy E_0 but decays; the gain and loss having exactly the same rates. The corresponding Hamiltonian, analogous to (4), can be written as

$$\hat{H} = \begin{pmatrix} E_0 + i\Gamma/2 & d \\ d & E_0 - i\Gamma/2 \end{pmatrix}, \tag{5}$$

where the real parameter d denotes coupling between the two states. Such Hamiltonians are called $\mathscr{P}\mathscr{T}$-symmetric, because they remain invariant under the combined action of parity interchanging the two states, $|1\rangle \leftrightarrow |2\rangle$, and of time reversal interchanging the gain with loss, $\Gamma \leftrightarrow -\Gamma$.

Computing eigenvalues and eigenvectors of the matrix (5), we obtain

$$E_\pm = E_0 \pm \sqrt{d^2 - \Gamma^2/4}, \qquad |\psi_\pm\rangle = \begin{pmatrix} 1 \\ \pm\sqrt{1 - (\Gamma/2d)^2} - i\Gamma/2d \end{pmatrix}. \tag{6}$$

We see that both eigenvalues are real if the intensity of gain and loss is not large, namely, $|\Gamma| < 2d$. In this case $| \pm \sqrt{1-(\Gamma/2d)^2} - i\Gamma/2d| = 1$ and, hence, the eigenvector is equally distributed between the gain $|1\rangle$ and loss $|2\rangle$ states. As a result, the loss balances gain and the mode amplitude stays constant. Otherwise, if $|\Gamma| > 2d$, both eigenvalues in (6) are complex: One of the eigenmodes decays and the other grows with time, because the eigenvectors are not distributed equally between the gain and loss states. At $|\Gamma| = 2d$, a non-Hermitian degeneracy is obtained, the so-called exceptional point, which will be described in the next section in more detail.

The fact that $\mathscr{P}\mathscr{T}$-symmetric Hamiltonians have a real spectrum follows from a more general concept of pseudo-Hermitian Hamiltonians [27]. The Hamiltonian $\hat{H}$ is called pseudo-Hermitian if there is an invertible Hermitian operator $\hat{\eta}$ such that

$$\hat{H}^\dagger \hat{\eta} = \hat{\eta}\hat{H}. \tag{7}$$

Such Hamiltonians are in general non-Hermitian, but they conserve the quantity

$$\langle \hat{\eta} \rangle = \langle \Psi(t)|\hat{\eta}|\Psi(t)\rangle, \tag{8}$$

where $\Psi(t)$ satisfies the Schrödinger equation $i\dot{\Psi} = \hat{H}\Psi$. This conservation property follows from (7) after differentiating $\langle \hat{\eta} \rangle$ with respect to time.

It is not difficult to see that the property of having a real spectrum is robust under small perturbations, as long as the Hamiltonian satisfies condition (7) and all its eigenvalues are non-degenerate. Indeed, let E be a non-degenerate real eigenvalue with the right eigenvector $|\psi_R\rangle$ and left eigenvector $\langle \psi_L|$:

$$\hat{H}|\psi_R\rangle = E|\psi_R\rangle, \qquad \langle \psi_L|\hat{H} = E\langle \psi_L|. \tag{9}$$

Note that, for non-Hermitian Hamiltonians, right and left eigenvectors are generally different, $|\psi_R\rangle \neq |\psi_L\rangle$; here we use the Dirac bra-ket notation and the definition of bra-states includes the conjugation $|\psi_L\rangle = \langle \psi_L|^\dagger$. In the case of a non-degenerate eigenvalue, the scalar product of left-right eigenvectors is nonzero, $\langle \psi_L|\psi_R\rangle \neq 0$, see e.g. [25, 33]. Using the properties $\hat{\eta}^\dagger = \hat{\eta}$, relation (7) written as $\hat{\eta}^{-1}\hat{H}^\dagger = \hat{H}\hat{\eta}^{-1}$ and the second equation in (9), we derive:

$$\hat{H}\hat{\eta}^{-1}|\psi_L\rangle = \left(\langle \psi_L|\hat{\eta}^{-1}\hat{H}^\dagger\right)^\dagger . = \left(\langle \psi_L|\hat{H}\hat{\eta}^{-1}\right)^\dagger = \left(E\langle \psi_L|\hat{\eta}^{-1}\right)^\dagger = E^*\hat{\eta}^{-1}|\psi_L\rangle. \tag{10}$$

We just have shown that, for any eigenvalue E, the complex conjugate E^* is the eigenvalue with the right eigenvector

$$|\psi_R'\rangle = \hat{\eta}^{-1}|\psi_L\rangle. \tag{11}$$

For a non-degenerate real eigenvalue, we have $E = E^*$, which implies the relation between the right and left eigenvectors as $|\psi_R\rangle \propto \hat{\eta}^{-1}|\psi_L\rangle$ (equality up to a

complex factor). Now we can see that a non-degenerate real eigenvalue cannot become complex under a small perturbation of the Hamiltonian, because otherwise a real eigenvalue E would split into a complex conjugate pair E and E^*; this is clearly in the contradiction to the assumption that E is non-degenerate. We see that the spectrum of the pseudo-Hermitian Hamiltonian remains real with a change of parameters until the point with a spectral degeneracy. As we will see in the next section, a typical degeneracy appearing in this case is the EP.

Let us define the parity operator as

$$\hat{P} = \begin{pmatrix} 0 & 1 \\ 1 & 0 \end{pmatrix}, \tag{12}$$

which interchanges the states $|1\rangle$ and $|2\rangle$ and, thus, its square $\hat{P}^2 = \hat{I}$ is the identity matrix. For the 2×2 matrix (5), condition (7) holds for $\hat{\eta} = \hat{P}$ as one can easily verify. In this case the conserved quantity (8) becomes $\langle\hat{\eta}\rangle = \varphi_1^*\varphi_2 + \varphi_2^*\varphi_1$, where $|\Psi(t)\rangle = \varphi_1(t)|1\rangle + \varphi_2(t)|2\rangle$. Note that $\langle\hat{\eta}\rangle$ is not positive definite, thus, its conservation does not necessarily imply that the solution is bounded. In fact, exponential growing or decaying solutions appear when $\Gamma > 2d$. Since the Hamiltonian (5) is complex and symmetric, Eqs. (9) for the right and left eigenvectors are transposed to each other and, hence, the eigenvectors are complex conjugate, $|\psi_L\rangle = |\psi_R^*\rangle$. From relation (11) we see that the eigenvector $|\psi_R'\rangle = \hat{P}|\psi_L\rangle = \hat{P}|\psi_R^*\rangle$ with the eigenvalue E^* describe the mode that is $\mathscr{P}\mathscr{T}$-symmetric to $|\psi_R\rangle$ and E.

For a complex symmetric Hamiltonian, let us introduce the c-product of two vectors ψ_1 and ψ_2 denoted by $(\psi_1|\psi_2)$ as [25, Ch. 6 and 9]

$$(\psi_1|\psi_2) = \langle\psi_1^*|\psi_2\rangle. \tag{13}$$

Here the complex conjugation in the first vector implies that $\langle\psi_1^*| = |\psi_1^*\rangle^\dagger = |\psi_1\rangle^T$ is only transposed, instead of Hermitian transposed. It is convenient to normalize the eigenvector of a non-degenerate eigenmode with this c-product as $(\psi_R|\psi_R) = 1$, which yields the eigenvector $|\psi_R\rangle$ defined up to a sign; note that this normalization is not possible for a degenerate eigenvalue, see Sect. 3. From the results of the previous paragraph it follows that the mode with a non-degenerate real eigenvalue $E = E^*$ is $\mathscr{P}\mathscr{T}$-symmetric, with the eigenvector satisfying the relation $|\psi_R\rangle = \pm\hat{P}|\psi_R^*\rangle$, where the sign distinguishes symmetric and anti-symmetric modes. In such a case (when the spectrum of the Hamiltonian is real), $\mathscr{P}\mathscr{T}$-symmetry is called exact. When eigenvalues of the Hamiltonian are complex, $\mathscr{P}\mathscr{T}$-symmetry is broken: each eigenmode with complex E is $\mathscr{P}\mathscr{T}$-symmetric to the complex conjugate mode with E^*.

Expression (5) provides a subset of all pseudo-Hermitian Hamiltonians for the choice $\hat{\eta} = \hat{P}$. This is, of course, not the only type of Hamiltonians that possess a real spectrum. For example, the Hamiltonian

$$\hat{H}' = \begin{pmatrix} -E_0 & id \\ id & E_0 \end{pmatrix}, \qquad d, E_0 \in \mathbb{R}, \tag{14}$$

is pseudo-Hermitian with $\hat{\eta} = \hat{P}'$, where

$$\hat{P}' = \begin{pmatrix} 1 & 0 \\ 0 & -1 \end{pmatrix}, \qquad (\hat{P}')^2 = \hat{I}. \tag{15}$$

This Hamiltonian is $\mathscr{P}\mathscr{T}$-symmetric with respect to the parity defined by $\hat{P}'$ (changing sign of the second state $|2\rangle$) and the time reversal interchanging the gain and loss, $ig \mapsto -ig$. At the same time, this Hamiltonian is anti-$\mathscr{P}\mathscr{T}$-symmetric with the parity operator (12) interchanging the states $|1\rangle$ and $|2\rangle$. We refer to [15, 29, 42] for physical applications of anti-$\mathscr{P}\mathscr{T}$-symmetric systems.

Furthermore, the relation between $\mathscr{P}\mathscr{T}$-symmetric and pseudo-Hermitian Hamiltonians extends in exactly the same form to multiple-state systems. The respective Hamiltonians are defined as $\hat{H} = \hat{H}_0 + i\hat{V}$ with the real symmetric matrices (or operators) $\hat{H}_0$ and $\hat{V}$, where $\hat{H}_0$ describes the Hermitian system and $\hat{V}$ provides the contribution due to gain and loss. The $\mathscr{P}\mathscr{T}$-symmetry imposes the additional conditions that $\hat{H}_0$ is symmetric and $\hat{V}$ is anti-symmetric under the parity transformation $\hat{P}$, i.e.,

$$\hat{P}\hat{H}_0 = \hat{H}_0\hat{P}, \qquad \hat{P}\hat{V} = -\hat{V}\hat{P}. \tag{16}$$

Such $\mathscr{P}\mathscr{T}$-symmetric Hamiltonians are also pseudo-Hermitian with $\hat{\eta} = \hat{P}$, since condition (7) with the complex symmetric operator $\hat{H} = \hat{H}_0 + i\hat{V}$ and real operator $\hat{P}$ reduces to the (anti-)commutation relations (16).

We stress again that $\mathscr{P}\mathscr{T}$-symmetry is only one of many ways to impose a real spectrum in a structurally stable way. For example, consider $\hat{H} = \hat{H}_0 + i\hat{V}$ with real symmetric operators $\hat{H}_0$ and $\hat{V}$. If $\hat{H}_0$ is invertible, one can take $\hat{\eta} = \hat{H}_0$. Then, condition (7) for the operator $\hat{H}$ to be pseudo-Hermitian reduces to the anticommutation relation $\hat{H}_0\hat{V} + \hat{V}\hat{H}_0 = 0$.

3 Exceptional Point at the Transition from a Real to a Complex Spectrum

Let us analyze the transition from a real to a complex spectrum for a simple $\mathscr{P}\mathscr{T}$-symmetric Hamiltonian (5). Its eigenvalues and eigenvectors are found explicitly in Eq. (6). Let us denote $\Gamma_{EP} = 2d$. For $\Gamma < \Gamma_{EP}$ the spectrum is real, while for $\Gamma > \Gamma_{EP}$ the spectrum is complex. At the transition point $\Gamma = \Gamma_{EP}$, the two eigenvalues and two eigenvectors coalesce at $E_+ = E_- = E_{EP}$ and $|\psi_+\rangle = |\psi_-\rangle = |\psi_{EP}\rangle$, where

$$E_{EP} = E_0, \qquad |\psi_{EP}\rangle = \begin{pmatrix} 1 \\ -i \end{pmatrix}. \tag{17}$$

The point with such properties (full coalescence of two eigenmodes both in their eigenvalues and eigenvectors) is called the *exceptional point* (EP). At the EP, the spectrum is incomplete in the sense that the eigenvectors do not constitute a full basis for the wave function. It is easy to see that the unique eigenvector at the EP is self-orthogonal with respect to the c-product (13):

$$(\psi_{EP}|\psi_{EP}) = 0. \tag{18}$$

In the language of linear algebra, the EP implies that the canonical Jordal form of the Hamiltonian contains a Jordan block [33]. The well-known property of the Jordan block is that its right and left eigenvectors (9) are orthogonal. For a symmetric Hamiltonian $\hat{H}$, this property is equivalent to the c-product self-orthogonality condition (13) because, at the EP, one has $|\psi_R\rangle = |\psi_{EP}\rangle$ and $\langle\psi_L| = |\psi_{EP}\rangle^T$.

The EP plays important role for the representation of spectrum in the form of Taylor series. Let us rewrite the Hamiltonian (5) in the form

$$\hat{H}(\lambda) = \hat{H}_0 + i\lambda\hat{V}, \tag{19}$$

where $\hat{H}_0 = E_0\hat{I} + d\hat{\sigma}_x$ and $\hat{V} = \hat{\sigma}_z$ with the Pauli matrices $\hat{\sigma}_x$ and $\hat{\sigma}_z$. The factor $\lambda = \Gamma/2$ describing the gain and loss will be considered as a perturbation parameter, with $\lambda = 0$ corresponding to the Hermitian Hamiltonian $\hat{H}(0) = \hat{H}_0$. Eigenvalues (6) of the Hamiltonian (19) can be written as

$$E_{\pm}(\lambda) = E_{EP} \pm \sqrt{\lambda_{EP}^2 - \lambda^2}, \qquad \lambda_{EP} = \Gamma_{EP}/2 = d. \tag{20}$$

They are analytic functions of λ with the branch point singularities at $\lambda = \pm\lambda_{EP}$. These functions can be expanded in the Taylor series

$$E_j(\lambda) = \sum_{n=0}^{\infty} C_j^{(n)}\lambda^n, \tag{21}$$

where $j = \pm$. The branch point λ_{EP} defines the radius of a circle in the complex parameter plane, $|\lambda| < \lambda_{EP}$, where the Taylor series (21) converges.

In the neighborhood of the EP, dependence of the eigenvalues on a parameter λ is shown in Fig. 1. According to expressions (20), the leading term of this dependence near λ_{EP} can be written as

$$E_{\pm}(\lambda) \approx E_{EP} \pm a\sqrt{\lambda - \lambda_{EP}}, \tag{22}$$

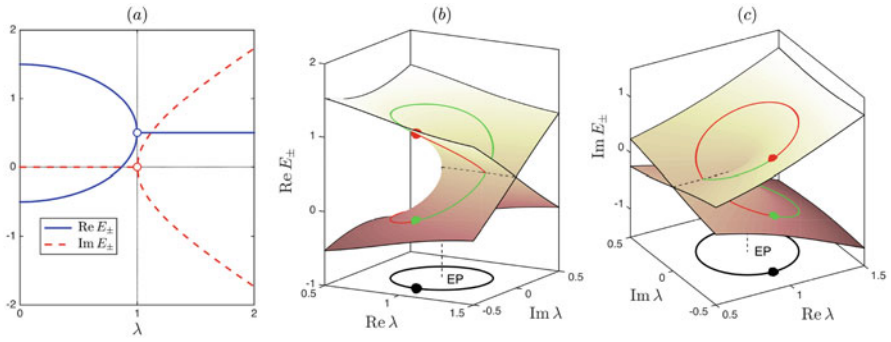

Fig. 1 (**a**) Real and imaginary parts of eigenvalues $E_\pm$ from (20) as functions of the real parameter λ; the numerical values are taken as $E_{EP} = 1/2$ and $\lambda_{EP} = 1$. Same graphs but as functions of the complex parameter λ are shown for (**b**) $\mathrm{Re}\, E_\pm$ with the intersection corresponding to $\mathrm{Re}\,\lambda > \lambda_{EP}$, $\mathrm{Im}\,\lambda = 0$ and (**c**) $\mathrm{Im}\, E_\pm$ with the intersection corresponding to $\mathrm{Re}\,\lambda < \lambda_{EP}$, $\mathrm{Im}\,\lambda = 0$. In horizontal projection, the black line describes the change of λ along a cycle around the EP. The corresponding change of two eigenvalues leading to the switch between two states is shown by the red and green curves. In one cycle of λ, the state E_- (green ball) is transported to the state E_+ (red ball), and vice versa

with the purely imaginary prefactor $a = i\sqrt{2\lambda_{EP}}$. Thus, the eigenvalues as functions of the real parameter λ have the square root singularity for both real and imaginary parts at λ_{EP}, see Fig. 1a. When extended to the complex values of λ, the local dependence is described by the two-sheet Riemann surface (branch point singularity) as shown in Fig. 1b, c.

One of the implications of the branch point singularity in Eq. (22) is that the two eigenmodes are interchanged when λ is changed continuously in the complex plane around the EP, see Fig. 1b, c. After the second cycle around the EP, the eigenvalues and eigenvectors return to their original values. This effect is known as the switch of eigenmodes for the parametric encircling of the EP, and it was observed experimentally in a microwave system [11]. In this experiment, the switch characterizes the eigenstates at different time-independent values of λ rather than the evolution of a wavefunction with λ changing in time. In fact, this switch mechanism does not work if the parameter λ is changed in time, i.e. for the dynamic encircling of the EP, because one of the transitions is always broken due to non-adiabatic effects. Although the adiabatic theorem does not hold, the topological property of the EP is manifested. When encircling the EP, the transitions acquire a chiral property: the final state depends on the direction in which the EP is encircled. We refer to [16, 17, 37] for the theory and physical applications, and to [12, 43] for the experimental observations of this effect. We stress that the system is not $\mathscr{PT}$-symmetric for complex values of λ. In general, a second-order degeneracy requires two real parameters in order to satisfy the single complex constraint, $E_1 = E_2$, at the EP. However, in $\mathscr{PT}$-symmetric systems, the EP can be found conveniently by tuning a single parameter, due to the reality of the spectrum below the symmetry-breaking point.

The described local properties of the EP extend similarly to systems with more than two states, when the $\mathscr{P}\mathscr{T}$-symmetric Hamiltonian has the form (19) with real symmetric operators $\hat{H}_0$ and $\hat{V}$ satisfying the (anti-)symmetry relations (16). In this case a large variety of spectral singularities may appear, including EPs (branch points) of higher order and eigenvalue crossings with distinct eigenvectors (so-called diabolic points); see e.g. [8, 25, 34]. For the higher-order EP, expansions for eigenvalues and eigenvectors of non-Hermitian Hamiltonians contain fractional powers like $(\lambda - \lambda_{EP})^{1/p}$ (the so-called Puiseux series), where p is the number of eigenvalues and eigenvectors that coalesce at the EP [25, Sections 7.7 and 9.1.1]; see also [24, 33] for the general perturbation theory and numerical methods. It should be stressed, however, that singularities in the spectrum of the generic (typical) $\mathscr{P}\mathscr{T}$-symmetric Hamiltonian with a single real parameter λ appear at discrete values, $\lambda = \lambda_j^{EP}$ $(j = 1, 2, \ldots)$, and have the form of the EPs with only two coalescent eigenvalues and eigenvectors [2]. In this case, the local behavior of eigenvalues and eigenvectors near the EP is equivalent (and in fact can be reduced) to the case of 2×2 Hamiltonian studied above. Note that such EPs must exist whenever the matrices $\hat{H}_0$ and $\hat{V}$ do not commute [26].

Finally, let us describe some properties of the Taylor expansions (21) for the eigenvalue E_j $(j = 1, \ldots, n)$ in the general case of $\mathscr{P}\mathscr{T}$-symmetric Hamiltonian operator (19). This expansion can be written as

$$E_j(\lambda) = \sum_{n=0}^{\infty} c_j^{(n)} \Lambda^n, \qquad c_j^{(n)} = (-i)^n C_j^{(n)}, \tag{23}$$

where $\Lambda = i\lambda$, $\hat{H} = \hat{H}_0 + \Lambda\hat{V}$, and we redefined the coefficients of (21) to include powers of the imaginary unit. Let us show that in $\mathscr{P}\mathscr{T}$-symmetric systems, all the odd coefficients vanish and all the even coefficients are real; therefore, the spectrum is real as long as the series converges. Since $\hat{H}_0$ and $\hat{V}$ are real symmetric matrices, one can use the Hermitian perturbation theory for real Λ, which is extended analytically to $\mathscr{P}\mathscr{T}$-symmetric Hamiltonians for purely imaginary Λ. From this argument, we immediately conclude that all the perturbational coefficients $c_j^{(n)}$ are real. Furthermore, from the Wigner $(2n + 1)$-rule [40] we express the odd-order coefficients as

$$c_j^{(2n+1)} = \langle \psi_j^{(n)} | \hat{V} | \psi_j^{(n)} \rangle, \tag{24}$$

where the real vector $|\psi_j^{(n)}\rangle$ is the nth-order correction in the expansion for the eigenvector

$$|\psi_j\rangle = \sum_{n=0}^{\infty} \Lambda^n |\psi_j^{(n)}\rangle. \tag{25}$$

Applying the parity operator to the equality $E|\psi_j\rangle = (\hat{H}_0 + \Lambda\hat{V})|\psi_j\rangle$, we obtain

$$E\,\hat{P}|\psi_j\rangle = \hat{P}(\hat{H}_0 + \Lambda\hat{V})|\psi_j\rangle = (\hat{H}_0 - \Lambda\hat{V})\hat{P}|\psi_j\rangle, \tag{26}$$

where we used the (anti-)symmetry assumptions (16). We see that $\hat{P}|\psi_j\rangle$ is the eigenvector corresponding to the parameter value $-\Lambda$. This means that the coefficients in the expansion (25) for Λ and $-\Lambda$ should match such that

$$P|\psi_j^{(n)}\rangle = \pm(-1)^n|\psi_j^{(n)}\rangle, \tag{27}$$

where the first sign depends whether the unperturbed real state $|\psi_j^{(0)}\rangle$ (at $\Lambda = 0$) is $\mathscr{P}$-symmetric or anti-symmetric (even or odd). Using the relations $\hat{P}^2 = \hat{I}$, (16) and (27) in (24), we obtain

$$c_j^{(2n+1)} = \langle\psi_j^{(n)}|\hat{V}|\psi_j^{(n)}\rangle = \langle\psi_j^{(n)}|\hat{P}^2\hat{V}\hat{P}^2|\psi_j^{(n)}\rangle = -c_j^{(2n+1)}, \tag{28}$$

i.e., all odd-order coefficients $c_j^{(2n+1)}$ vanish. With this property, we showed explicitly that the spectrum of the $\mathscr{P}\mathscr{T}$-symmetric Hamiltonian $\hat{H}$ is real as long as the series (23) is convergent, i.e.

$$|\lambda| < \min_j |\lambda_j^{EP}| \tag{29}$$

for the minimum among all EPs.

4 $\mathscr{P}\mathscr{T}$−Symmetric System of Coupled Waveguides Near the EP

We will show in this section that a system of two coupled waveguides (WGs) can be made $\mathscr{P}\mathscr{T}$-symmetric if the gain in one WG is accurately balanced by the loss in the second WG. In this setup, the EP appears for a specific value of the gain-loss parameter. In our description we follow the theoretical work of one of us together with Shachar Klaiman and Uwe Günter [21]. The effects we describe were first observed in the experiments conducted in the Laboratory of Detlef Kip together with Mordechai Segev and members of the group of Demetrios N. Christodoulides [31].

A $\mathscr{P}\mathscr{T}$-symmetric optical system can be easily realized with a symmetric index guiding profile and an antisymmetric gain and loss profile, i.e., $n(x) = n^*(-x)$ [13]. We consider two coupled planar WGs depicted in Fig. 2 for which the refractive index varies only in the x-direction. The direction of propagation in the WGs is taken to be the z-axis. The wave equation for the transverse-electric (TE) modes (derived from the full Maxwell equations) reads [20]:

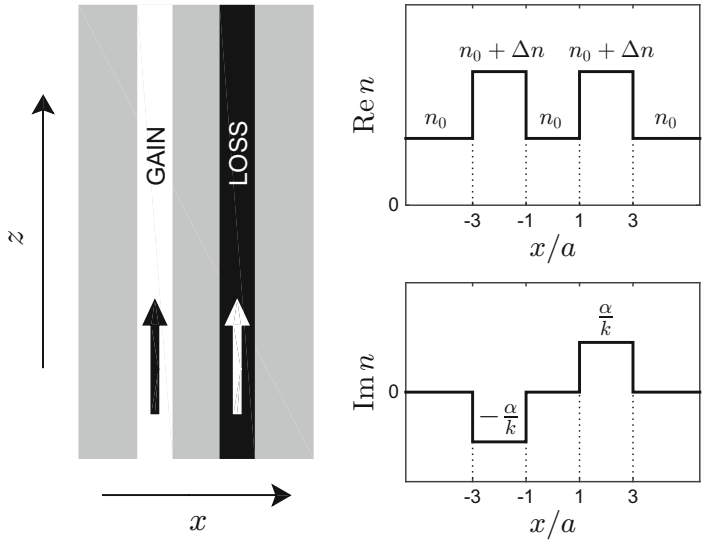

Fig. 2 Coupling between the gain guided mode and the loss guided mode provides a $\mathscr{P}\mathscr{T}$-symmetric system with the refractive index profile such that $n(x) = n^*(-x)$. A control parameter α defines the gain and loss strength in the WGs as $\mathrm{Im}\, n = \pm\alpha/k$. The refractive index only varies in the x direction

$$\frac{\partial^2\psi}{\partial x^2} + \left(\frac{n(x)^2\omega^2}{c^2} - \beta^2\right)\psi = 0, \tag{30}$$

where the y-component of the electric field is given by

$$E_y(x, z, t) = \psi(x)e^{i(\omega t - \beta z)}. \tag{31}$$

Here β is the propagation constant and ω is the frequency. The vacuum wavelength is equal to $2\pi/k$ with $k = \omega/c$. Clearly, the wave equation (30) for the y-component of the electric field is analogous to the one-dimensional Schrödinger equation:

$$\left(-\frac{1}{2}\frac{\partial^2}{\partial x^2} + V(x)\right)\psi(x) = E\psi(x), \tag{32}$$

identifying $V(x) = -k^2n^2(x)/2$ as the potential, $E = -\beta^2/2$ as the energy, and $\psi(x)$ as the wave function.

As shown in Fig. 2, we couple between one gain-guiding WG (negative imaginary part of the refractive index) and one loss-guiding WG (positive imaginary part of the refractive index) in order to create the $\mathscr{P}\mathscr{T}$-symmetric structure [35]. For simplicity we take the separation between the two coupled WGs to be the same as the their width, i.e., $2a$. Note that in our case the imaginary part of refractive

index (the complex part of potential) vanishes as $x \to \pm\infty$. For propagating modes (bound states), we impose the boundary conditions $\psi(x) \to 0$ as $x \to \pm\infty$.

For the numerical illustration, we choose the following parameters for the WG structure shown in Fig. 2. The background index is taken to be $n_0 = 3.3$, the vacuum wavelength $2\pi/k = 1.55\,\mu\text{m}$, the real index difference between the WGs and the background material $\Delta n = 10^{-3}$, and the separation between the WGs, which equals the WGs width, $2a = 5\mu\text{m}$. The imaginary part of the refractive index in the WGs is chosen as $\text{Im}\, n = \pm\alpha/k$, where α is a parameter. The parameters are chosen such that each WG contains only a single guided mode before we couple them. The coupled guided modes are calculated by diagonalizing the matrix representation of Eq. (30) in a sine basis. The resulting "Hamiltonian" matrix is non-Hermitian and one needs to take care when normalizing the eigenvectors. We choose to normalize our eigenvectors according to the c-product (13), i.e., $(\psi_n|\psi_m) = \langle\psi_n^*|\psi_m\rangle = \delta_{n,m}$.

The coupled waveguides support two guided modes. The propagation constants of the two modes are plotted in Fig. 3 as functions of the gain-loss parameter α. Increasing α causes the propagation constants of the two modes to move towards each other and coalesce at $\alpha_{EP} \approx 8.4\,\text{cm}^{-1}$. As long as $\mathscr{P}\mathscr{T}$ symmetry remains exact, i.e. $\alpha < \alpha_{EP}$, the power of each guided mode is distributed equally between the two WGs. The critical value α_{EP} is the EP, where the two modes coalesce: both the propagation constants and the corresponding electric fields become equal. Therefore, one can study the EP in a $\mathscr{P}\mathscr{T}$-symmetric WG system by varying only a single gain-loss parameter α. Past the critical value, $\alpha > \alpha_{EP}$, the propagation

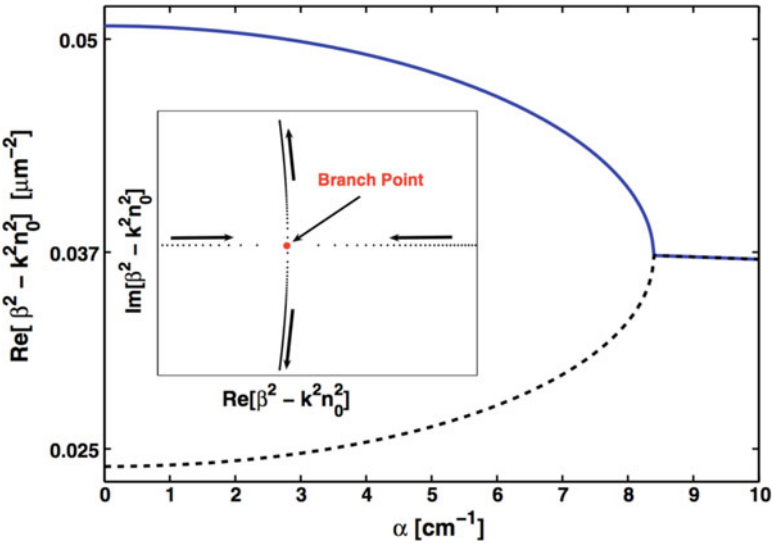

Fig. 3 Two trapped modes of the WGs of Fig. 2 as functions of the gain-loss parameter α. The eigenmodes approach each other on the real axis as α increases until a critical value of $\alpha_{EP} \approx 8.4\,\text{cm}^{-1}$. The critical value is the EP (branch point), where the two modes coalesce. Beyond the EP, the directional coupler sustains one gain guiding mode and one loss guiding mode

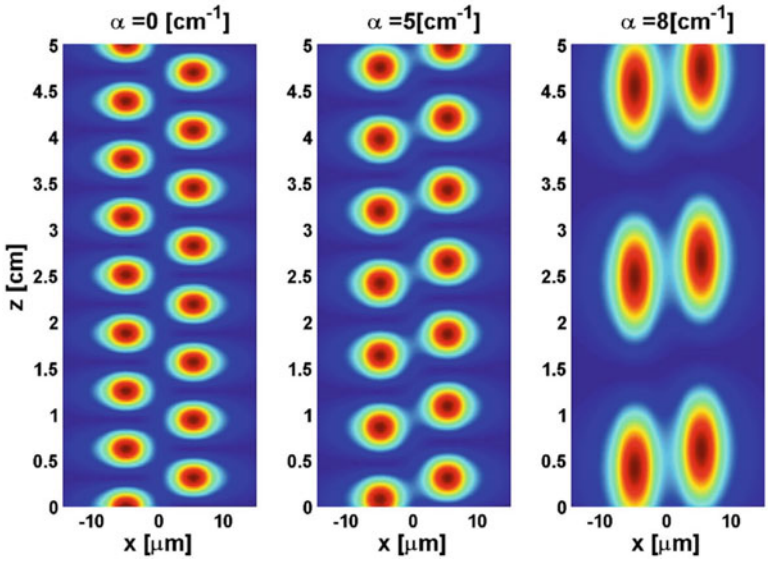

Fig. 4 The power distribution for a propagating sum field consisting of the two guided modes, see Eq. (33) for three values of α. As can be readily observed, the beat length (analogous to the beat time period in quantum mechanics) increases as the value of α approaches the critical value $\alpha_{EP} \approx 8.4\,\mathrm{cm}^{-1}$

constants become complex conjugate to each other. Then the WGs support one gain-guiding mode and one loss-guiding mode. The corresponding transverse field no longer retains the symmetry properties of the $\mathscr{P}\mathscr{T}$ operator, but rather each of the two modes becomes localized in one of the waveguides.

The advance of two real propagation constants towards the EP can be visualized by observing the beat length of the sum field for two equally populated modes:

$$E_y(x,z,t) = \frac{1}{\sqrt{2}}\left(\psi_1(x)e^{-i\beta_1 z} + \psi_2(x)e^{-i\beta_2 z}\right)e^{i\omega t}. \tag{33}$$

Figures 4 and 5 display the power distribution $|E_y(x,z,t)|^2$ for three values of α. One can see that the beat length, which is equal to $L = 2\pi/|\beta_2 - \beta_1|$, increases as α approaches the EP. At the EP, the sum field no longer oscillates between the two waveguides but rather travels in both waveguides simultaneously. This fact can be used for a direct observation of the EP: the propagation constants approach when the gain-loss parameter α is increased to the value at the EP. Recall that the critical value α_{EP} characterizes the maximum antisymmetric index profile, which can still be treated within perturbation theory; see Sect. 3.

Although propagation constants of the studied $\mathscr{P}\mathscr{T}$-symmetric WGs are real, the system is non-Hermitian. This can be most readily observed by looking at the integrated intensity, $\int_{-\infty}^{\infty}|E_y(x,z)|^2dx$. This intensity is not conserved as one can

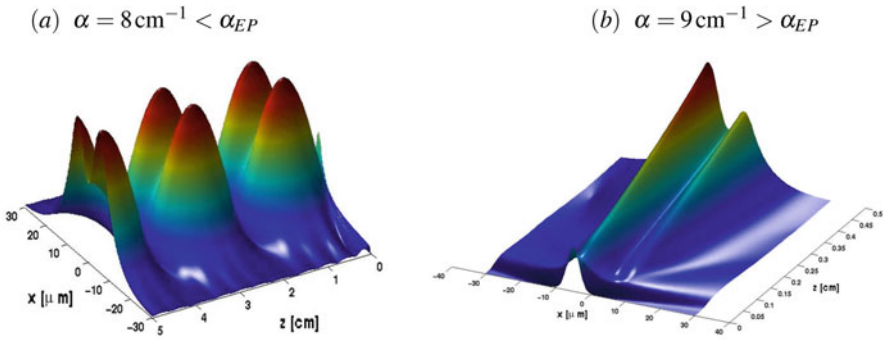

Fig. 5 3D representation of the power distribution for a propagating sum field (33). (**a**) The exact $\mathscr{P}\mathscr{T}$ symmetry with $\alpha = 8\,\mathrm{cm}^{-1} < \alpha_{EP}$. The light power oscillates, with the beat length increasing as the system approaches the EP at $\alpha_{EP} \approx 8.4\,\mathrm{cm}^{-1}$. (**b**) The broken $\mathscr{P}\mathscr{T}$ symmetry with $\alpha = 9\,\mathrm{cm}^{-1} > \alpha_{EP}$. The light power increases along the propagation axis, because the signal occupies primarily the WG with a gain-guiding mode

easily see from Figs. 4 and 5a: the intensity drops almost to zero between oscillations for $\alpha = 8\,\mathrm{cm}^{-1}$. In the case of $\mathscr{P}\mathscr{T}$-symmetric system, one can find a different conserved quantity instead of the integrated intensity; see Eq. (8) in Sect. 2. In our system, this conserved quantity takes the form of the c-product as

$$\int_{-\infty}^{\infty} E_y^*(-x, z) E_y(x, z) dx = const. \tag{34}$$

Yet another effect can be observed in the suggested experiment: the maximum intensity reached by the initially normalized sum field (33) increases as the EP is approached. This can be understood by observing that as one approaches the self-orthogonal state the overlap between the two functions comprising the sum field increases. Finally, Fig. 5b gives an insight on the dramatic change of light propagation when the gain-loss parameter exceeds the EP and the propagation constant gets a nonzero imaginary part.

It is important to note that the manifestation of $\mathscr{P}\mathscr{T}$ symmetry and its resulting properties is not (theoretically) restricted to optical systems. To date, however, optical systems seem to be the most readily applicable and $\mathscr{P}\mathscr{T}$ symmetry in optics was quoted among top 10 physics discoveries of the last 10 years by Nature Physics [10]. One could easily envision a setting using matter waves in which a condensate is placed in a double well potential, where in one well particles are injected into the condensate whereas in the second well particles are removed from the condensate. Here attention should be given to the non-linearity of the Gross-Pitaevskii equation. In order to keep the dynamics similar to that described in the optics experiment, the non-linearity should be made small. This can be achieved either by tuning the interaction between the atoms to zero or by using a very dilute sample. The experiment would also require accurate and independent control over

the rates of particles injected or removed from the system. Hopefully, experimental methods will improve to allow such experiments to be done.

5 Vanishing Group Velocity at the Exceptional Point

In this section, following our work with Tamar Goldzak [18], we extend the study of $\mathscr{P}\mathscr{T}$-symmetric WGs to the case of isolated wave pulses. We consider two-dimensional WGs with the propagation axis z described in the previous section. In a $\mathscr{P}\mathscr{T}$-symmetric system, the gain and loss are balanced and satisfy the condition $n(x) = n^*(-x)$, where the complex conjugation corresponds to the time reversal that interchanges the gain and loss. Equation (30) for transverse electric modes (31) is equivalent to the one-dimensional stationary Schrödinger equation (32) for the complex (non-Hermitian) potential, and the propagating modes correspond to bound states [25].

As long as the strength of gain and loss is below a problem dependent critical value (see Sect. 2), non-decaying modes exist with real propagation constants β. The corresponding complex eigenfunctions (by selecting a proper complex pre-factor) can be taken $\mathscr{P}\mathscr{T}$-symmetric, $\psi(x) = \psi^*(-x)$. Thus, the phase speed of each mode is defined as $v_p = \omega/\beta$, while the group speed is $v_g = (d\beta/d\omega)^{-1}$. For a nondegenerate bound-state solution, differentiating equation (30) with respect to ω yields

$$\left(\frac{\partial^2}{\partial x^2} + \frac{n^2\omega^2}{c^2} - \beta^2\right)\frac{\partial\psi}{\partial\omega} + \left(\frac{\partial(n^2\omega^2/c^2)}{\partial\omega} - \frac{\partial\beta^2}{\partial\omega}\right)\psi = 0. \tag{35}$$

Following the classical perturbation theory [23, 25], one multiplies this expression by $\psi(x)$ and integrates with respect to x. The terms with $\partial\psi/\partial\omega$ cancel in the resulting expression after integrating by parts and using (30). The remaining terms yield expression for the group speed as

$$v_g = (d\beta/d\omega)^{-1} = \frac{2c^2\beta\int\psi^2 dx}{\int[\partial(n^2\omega^2)/\partial\omega]\psi^2 dx}. \tag{36}$$

By the derivation, this formula takes into account that the index of refraction may be frequency dependent in general.

The numerator in (36) represents the c-product (13) of the right eigenfunction $|\psi_R\rangle = \psi(x)$ with itself. Due to the $\mathscr{P}\mathscr{T}$-symmetry, $\psi(x) = \psi^*(-x)$, the full integral $\int\psi^2 dx$ is real but not necessarily positive. For the same reason, the denominator is real too. It follows from Eq. (36) that the group speed vanishes if and only if $\int\psi^2 dx = 0$, provided that the integral in the denominator is nonzero. The latter condition is generic and can be easily verified in each specific problem. The c-product self-orthogonality of the propagating mode is the well-known condition for the exceptional point (EP); see Eq. (18). At the EP, two propagating modes coalesce

both in propagation constants β and corresponding functions $\psi(x)$. This proves that *the group speed in a $\mathscr{P}\mathscr{T}$-symmetric WG vanishes at (and only at) an exceptional point*. Such a simple and universal condition provides a link from $\mathscr{P}\mathscr{T}$-symmetric systems to the rapidly developing field of slow light; see [3, 4, 9, 19] for other ways to stop/slow light such as the electromagnetically induced transparency (EIT).

According to Sect. 3, expansion of eigenvalues near the EP starts with a square root term

$$\beta - \beta_{EP} \propto \sqrt{\omega - \omega_{EP}}, \tag{37}$$

which implies that $d\beta/d\omega = \infty$ and $v_g = (d\beta/d\omega)^{-1} = 0$ at the EP. This provides a simple explanation of our phenomenon, because a steep slope in the dispersion curve (large derivative $d\beta/d\omega$) corresponds to a small group velocity. This argument relies exclusively on the presence of the EP, with no reference of $\mathscr{P}\mathscr{T}$-symmetry. The problem is that in conventional systems this effect will also lead to losses. The balance between gain and loss in a $\mathscr{P}\mathscr{T}$ symmetric system eliminates this problem: the light intensity remains constant because the spectrum is real (before reaching the EP). Also, the real spectrum of the $\mathscr{P}\mathscr{T}$ symmetric system simplifies a definition of the group speed, which is a nontrivial issue for a general system with gain and loss. The direct link between the EP and zero group speed makes the proposed effect robust to various imperfections, as the proximity to the EP can be effectively controlled by tuning two arbitrarily chosen parameters of the system [25, 33]. The stopping condition is limited to a very well defined EP frequency ω_{EP}. Its value can be effectively controlled by changing the parameters of the index of refraction.

We mention also that the EPs may appear in a different context: at the coalescing frequencies of Bloch modes for the (time-periodic) Schrödinger equation. Such EPs can be associated with the infinite group speed in corresponding optical systems [32]; see [38, 41] for physical interpretation of the superluminal effect.

A specific device with desired properties can be constructed by attaching layers of materials with different indices of refraction. The refractive index can be engineered, e.g., via the photorefractive nonlinearity or effective index as in metamaterials, while the spectrum of gain/loss can be engineered by using quantum well structures. The $\mathscr{P}\mathscr{T}$-symmetry is achieved if one gain guided mode (negative $\mathrm{Im}\, n$) couples with an exactly balanced loss guided mode (positive $\mathrm{Im}\, n$) [21, 35], with a profile of the refractive index shown in Fig. 2. Note that the standard gain media are dispersive, i.e., the index of refraction is frequency dependent. This frequency dependence may break the $\mathscr{P}\mathscr{T}$ symmetry due to a finite gain bandwidth.

Let us describe the effective light intensities of the two (gain and loss) modes by two complex variables (φ_1, φ_2). Then one obtains a simple model in the form of 2×2 $\mathscr{P}\mathscr{T}$-symmetric non-Hermitian system

$$\begin{pmatrix} \beta_w^2 - i\widetilde{\alpha}k & \delta \\ \delta & \beta_w^2 + i\widetilde{\alpha}k \end{pmatrix} \begin{pmatrix} \varphi_1 \\ \varphi_2 \end{pmatrix} = \beta^2 \begin{pmatrix} \varphi_1 \\ \varphi_2 \end{pmatrix}, \tag{38}$$

where the Hamiltonian has the same structure, up to notation, as in Eq. (5). Here $\beta_w = n_w k$ is the real propagation constant of each separate WG with the effective index of refraction n_w and $k = \omega/c$, δ describes the coupling, and $\widetilde{\alpha} = 2n_w\alpha$ determines the gain in one WG and the loss in the other. The system with no gain/loss ($\widetilde{\alpha} = 0$) has one symmetric and one antisymmetric mode, with $\beta^2 = \beta_w^2 \pm \delta$ and $(\varphi_1, \varphi_2) = (\pm 1,\ 1)$. When gain and loss are taken into account, one finds $\beta^2 = \beta_w^2 \pm \sqrt{\delta^2 - \widetilde{\alpha}^2 k^2}$. With increasing $\widetilde{\alpha}$, the real propagation constants come closer and coalesce at the EP given by $\widetilde{\alpha}_{EP} = \delta/k$. The corresponding two eigenvectors coalesce too, with the resulting vector $(\varphi_1, \varphi_2) = (1, i)$ satisfying the c-product self-orthogonality condition $\varphi_1^2 + \varphi_2^2 = 0$.

The full-stop of a Gaussian pulse can be accomplished by an adiabatic increase of the gain-loss parameter to the value $\widetilde{\alpha}_{EP}$, as was also proposed in the context of photonic-crystal waveguides [36, 44]. Varying the gain-loss parameter in our non-Hermitian system would be best done via parametric nonlinear gain, which separates the variation in the gain from affecting the real part of refractive index, avoiding restrictions imposed by the Kramers–Kronig relations. Nonlinear parametric interactions operating at ultrafast rates [39] can be engineered using synchronously-pumped optical parametric oscillators, where the nonlinear medium is in a cavity and pumped with a pulse at repetition rate matched to cavity, or optical parametric amplifiers pumped without a cavity by femtosecond pulse. Usually these utilize $\chi^{(2)}$ crystals, which are commercial technologies. Another choice is $\chi^{(3)}$ materials, through non-degenerate four-wave-mixing interactions, where the pumps serve as gain for the signal beams [1].

Time-dependent solutions for the simplified model (38) can be found using the system of coupled wave equations

$$\begin{aligned} \frac{n_w^2}{c^2}\frac{\partial^2\Phi_1}{\partial t^2} - \frac{\widetilde{\alpha}}{c}\frac{\partial\Phi_1}{\partial t} - \delta\,\Phi_2 - \frac{\partial^2\Phi_1}{\partial z^2} = 0, \\ \frac{n_w^2}{c^2}\frac{\partial^2\Phi_2}{\partial t^2} + \frac{\widetilde{\alpha}}{c}\frac{\partial\Phi_2}{\partial t} - \delta\,\Phi_1 - \frac{\partial^2\Phi_2}{\partial z^2} = 0. \end{aligned} \tag{39}$$

It is straightforward to check that this system is equivalent to Eq. (38) for a single-mode solution

$$(\Phi_1, \Phi_2) = (\varphi_1, \varphi_2)\, e^{i\beta z - i\omega t}. \tag{40}$$

Furthermore, it is easy to see that the model is $\mathscr{P}\mathscr{T}$-symmetric under the transformation:

$$\Phi_1(z,t) \to \Phi_2(-z,-t), \qquad \Phi_2(z,t) \to \Phi_1(-z,-t). \tag{41}$$

System (39) was simulated numerically using the pseudo-spectral method in a large periodic domain. Initial condition at $t = 0$ was taken in the form of a Gaussian pulse corresponding to the antisymmetric mode of the system with no gain and loss,

$$(\Phi_1, \Phi_2) = (-1, 1)\, A \int \exp\left(-\frac{(\beta-\beta_0)^2}{2\sigma^2} + i\beta z\right) d\beta, \tag{42}$$

with mean propagation constant $\beta_0 = 0.8$, standard deviation $\sigma = 0.01$ and arbitrary prefactor A. This value $\beta_0 = 0.8$ corresponds to the EP at the final time when $\widetilde{\alpha}_{EP} = 1$, see Fig. 6a. In simulations, we used a finite window $0.75 \leq \beta \leq 0.85$ to avoid instabilities, which occur for some propagation constants outside this interval. In practical applications, such instabilities (if they appear) must be suppressed for efficient operation of the system.

Numerical simulation of such time-dependent dynamics with the model (39) is presented in Fig. 6, where a Gaussian pulse is prepared initially in the antisymmetric mode of the system with no gain and loss. In full agreement with our theoretical prediction, with the increase of the gain-loss parameter in time, the pulse slows down and stops at the EP (graphs at latest times collapsed to a single curve). A backward change of the gain-loss parameter brings the signal to its original mobile form.

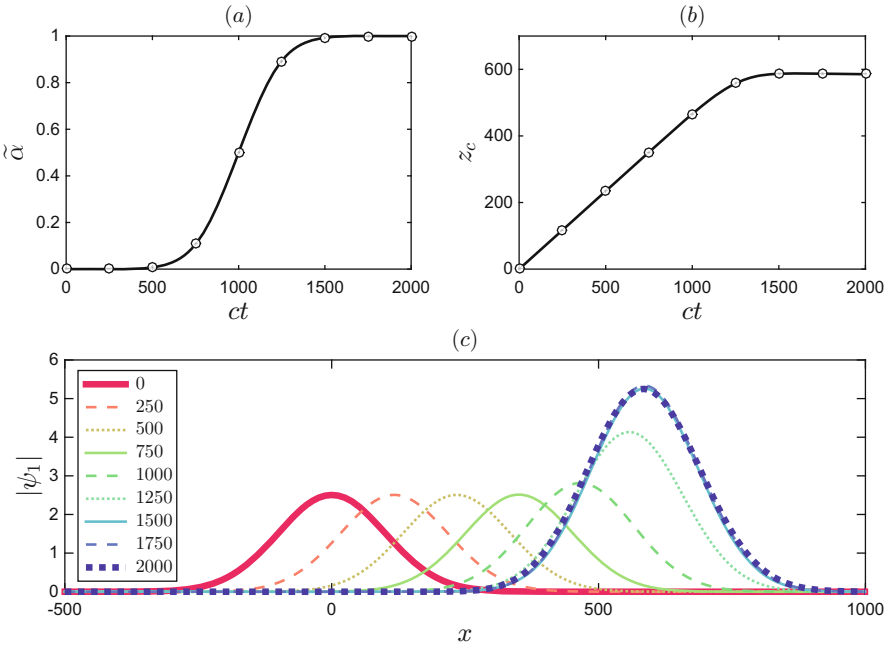

Fig. 6 (**a**) Adiabatic change of the gain-loss parameter from $\widetilde{\alpha} = 0$ at $t = 0$ to $\widetilde{\alpha}_{EP} = 1$ at final time $t = 2000/c$ in a system with representative parameters $k = 0.5$, $n_w = 1.6$, and $\delta = 0.5$ (arb. unit). (**b**) Temporal evolution of the center z_c of the Gaussian pulse, stopping when $\widetilde{\alpha}$ reaches the value $\widetilde{\alpha}_{EP} = 1$ at EP. The pulse is prepared initially in anti-symmetric mode of the system with no gain and loss with the mean propagation number $\beta = 0.8$ and standard deviation $\sigma = 0.01$. (**c**) Pulse envelope $|\Phi_1|$ in the first WG at times $ct = 0, 250, \ldots, 2000$, which correspond to circles in the upper figures. At the three latest times, the group speed vanishes and the corresponding graphs collapse to a single curve demonstrating the full-stop of a pulse. A backward change of the gain-loss parameter brings the optical signal to its original mobile form

Conclusions based on the effective model (38) are further confirmed by numerical computation for the full Eq. (30). Here the propagation constants β and eigenfunctions $\psi(x)$ are calculated numerically for given frequency ω by diagonalizing the non-Hermitian Hamiltonian in a matrix representation using a particle in a box basis set. We use specific values of the WG width $a = 1.25\,\mu\text{m}$ and the same distance between them. The two modes coalesce at the EP for specific values of k and β in the presence of gain and loss, and one can see from Fig. 7a that the derivative $d\beta/dk$ becomes infinite at the EP giving the vanishing group velocity $v_g = c\,(d\beta/dk)^{-1}$. The corresponding self-orthogonal eigenfunction is given in panel (b).

Finally, Fig. 8 shows the propagation of Gaussian wave packets, comparing the power spectrum $|E_y(x, z, t)|^2$ at the initial time $t = 0$ vs. the final time of 10 picoseconds. Here the Gaussian solution for a constant gain-loss parameter α is written as

$$E_y(x, z, t) = A \int \exp\left(-\frac{(\beta - \beta_0)^2}{2\sigma^2} + i\beta z - i\omega t\right) \psi(x) d\beta, \tag{43}$$

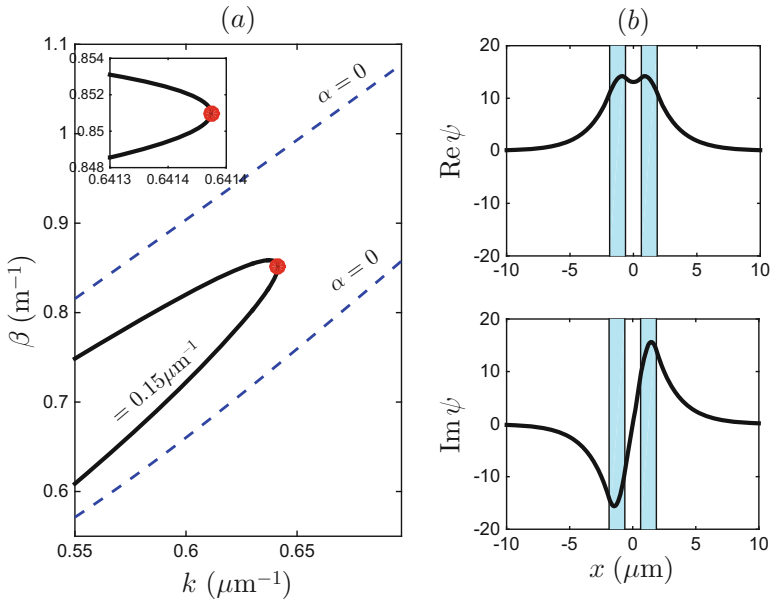

Fig. 7 (**a**) The propagation constant β as a function of $k = \omega/c$ for two different values of the gain-loss parameter: Hermitian system with $\alpha = 0$ (dashed black lines: upper symmetric and lower antisymmetric modes) and non-Hermitian $\mathscr{P}\mathscr{T}$-symmetric system with $\alpha = 0.15\,\mu\text{m}^{-1}$ (solid blue line). Two modes of the $\mathscr{P}\mathscr{T}$-symmetric system coalesce at the EP marked with a red circle. Inset shows enlarged vicinity of the EP at $k_{EP} = 0.6414\,\mu\text{m}^{-1}$ and $\beta_{EP} = 0.851\,\mu\text{m}^{-1}$. The infinite derivative $d\beta/dk$ at the EP yields the vanishing group velocity $v_g = c\,(d\beta/dk)^{-1}$. (**b**) Real and imaginary parts of the complex eigenfunction for the $\mathscr{P}\mathscr{T}$-symmetric system at the EP. This mode satisfies the self-orthogonality condition $\int \psi^2 dx = 0$. Colored vertical regions in the background show positions of the two coupled WGs

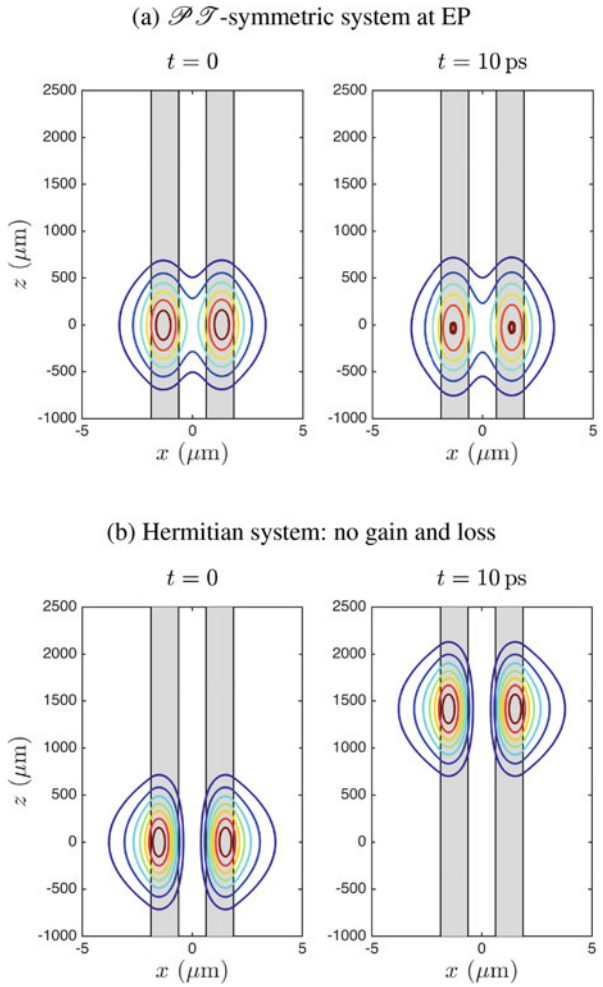

Fig. 8 Contour plot of the light power $|E_y(x, z, t)|^2$ for the Gaussian wave packets at the initial time $t = 0$ and the final time $t = 10\,\mathrm{ps}$. In both plots the pulse has the mean propagation constant $\beta = 0.851\,\mu\mathrm{m}^{-1}$ with standard deviation $\sigma = 0.002\,\mu\mathrm{m}^{-1}$. Grey regions in the background show positions of the two coupled WGs. (**a**) Fully stopped pulse centered exactly at the EP in the $\mathscr{P}\mathscr{T}$-symmetric system for $\alpha = 0.15\,\mu\mathrm{m}^{-1}$. (**b**) The antisymmetric mode in the Hermitian case with no gain and loss ($\alpha = 0$). One can see that the pulse is displaced by about 1.4 mm in the Hermitian case, while it does not move at all when prepared at the EP in the $\mathscr{P}\mathscr{T}$-symmetric system. (**a**) $\mathscr{P}\mathscr{T}$-symmetric system at EP. (**b**) Hermitian system: no gain and loss

where both ω and $\psi(x)$ should be expressed as functions of β. Note that the Gaussian pulse at the EP contains the contributions from both sides of β_{EP}, which correspond to two different modes coalescing at the EP in Fig. 7a. In numerical computations, we used $\beta_0 = 0.851\,\mu\text{m}^{-1}$, $\sigma = 0.002\,\mu\text{m}^{-1}$ and the overall interval $0.845 \le \beta \le 0.857\,\mu\text{m}^{-1}$. In Fig. 8a, the pulse parameters are chosen exactly at the EP, while figure (b) corresponds to a similar pulse but for the system far from the EP (no gain and loss, $\alpha = 0$). The latter pulse has the large group speed $v_g/c = 0.47$ and the phase speed $v_p/c = 0.82$, demonstrating a considerable displacement of about 1.4 mm in 10 ps, while the full-stop is confirmed for the pulse designed at the EP. We used illustrative values of physical parameters in these simulations, which provide a larger frequency window near the EP than those studied experimentally in [31]. Note that the dispersion curve in Fig. 7a exhibits a round shape including also a point with infinite group velocity [38, 41], where $d\beta/dk = 0$. This point is outside the operation window for our protocol.

The stopped signal in our system has the phase velocity $v_p/c = 0.75$, which is only weakly affected as the group velocity is reduced to zero under the EP mechanism. Furthermore, the phase speed demonstrates a slight decrease compared to the system with no gain and loss, contrary, e.g., to the well-known relation $v_p \propto 1/v_g$ in special relativity or in optics at the mode-opening.

The major advantages of the proposed protocol is its non-resonant nature, in which the EP can be adjusted to any frequency by tuning the coupling or gain-loss parameters. There is also a benefit of using the time-dependent variation of parameters. In this case an optical pulse is expanded in spatial Fourier modes with the frequency evolving adiabatically along the real dispersion curve in Fig. 7a. In this way our protocol avoids the instability related to complex modes at frequencies above the EP, as confirmed by our numerical tests in Fig. 6.

We see that the full-stop of a light pulse is possible at the exceptional point in $\mathscr{P}\mathscr{T}$-symmetric coupled waveguides by varying the gain-loss parameter in time. This allows to "freeze" and then release the light pulse preserving the carried coherent information. The use of $\mathscr{P}\mathscr{T}$-symmetry has practical advantages of keeping a constant intensity of propagating modes and providing a robust protocol that brings the system to the EP. The non-resonant mechanism of the proposed phenomenon, due to large flexibility of controlling the EP position, is an important technological advantage, with potential applications for short optical pulses. Specifically, one can engineer this effect in a $\mathscr{P}\mathscr{T}$-symmetric system of two waveguide channels. This approach is not limited only to light but can be extended, e.g., to acoustic waves or other fields in physics related to the $\mathscr{P}\mathscr{T}$-symmetry.

6 Conclusion

The transition from a real to a complex spectrum of non-Hermitian $\mathscr{P}\mathscr{T}$-symmetric Hamiltonians occurs at the exceptional point (EP), where two eigenmodes coalesce both in eigenvalue and eigenvector. In spite of the fact that EPs are accidental non-

Hermitian degeneracies they are not rare and not mathematical objects but physical ones. We have described in detail how light oscillations between two waveguides are suppressed by approaching the EP condition. We also prove that the group velocity of a light pulse decreases to zero as the system is tuned to be at the EP and propose a way how to observe it experimentally. Last but not least, the findings and conclusions presented in this Chapter are relevant to any two atomic or molecular metastable states, which are resonantly coupled by a laser field, because their non-Hermitian Hamiltonian can be simply transformed to have the $\mathscr{P}\mathscr{T}$-symmetric structure.

Acknowledgements The authors thank Adi Pick for most helpful comments. N.M. acknowledges the financial support of I-Core: The Israeli Excellence Center "Circle of Light", and of the Israel Science Foundation Grant No. 1530/15. A.A.M. was supported by the CNPq Grant No. 302351/2015-9.

References

1. Agrawal, G.P.: Nonlinear Fiber Optics. Academic, Amsterdam (2013)
2. Arnold, V.I.: Geometrical Methods in the Theory of Ordinary Differential Equations. Springer Science & Business Media, New York (2012)
3. Baba, T.: Slow light in photonic crystals. Nat. Photonics **2**(8), 465–473 (2008)
4. Bajcsy, M., Zibrov, A.S., Lukin, M.D.: Stationary pulses of light in an atomic medium. Nature **426**(6967), 638–641 (2003)
5. Bender, C.M.: Making sense of non-Hermitian Hamiltonians. Rep. Prog. Phys. **70**(6), 947 (2007)
6. Bender, C.M., Boettcher, S.: Real spectra in non-Hermitian Hamiltonians having PT symmetry. Phys. Rev. Lett. **80**(24), 5243 (1998)
7. Bender, C.M., Berry, M.V., Mandilara, A.: Generalized PT symmetry and real spectra. J. Phys. A **35**(31), L467 (2002)
8. Berry, M.V., Dennis, M.R.: The optical singularities of birefringent dichroic chiral crystals. Proc. R. Soc. A **459**(2033), 1261–1292 (2003)
9. Boyd, R.W., Gauthier, D.J.: Controlling the velocity of light pulses. Science **326**(5956), 1074–1077 (2009)
10. Cham, J.: Top 10 physics discoveries of the last 10 years. Nat. Phys. **11**(10), 799 (2015)
11. Dembowski, C., Gräf, H.D., Harney, H.L., Heine, A., Heiss, W.D., Rehfeld, H., Richter, A.: Experimental observation of the topological structure of exceptional points. Phys. Rev. Lett. **86**(5), 787–790 (2001)
12. Doppler, J., Mailybaev, A.A., Böhm, J., Kuhl, U., Girschik, A., Libisch, F., Milburn, T.J., Rabl, P., Moiseyev, N., Rotter, S.: Dynamically encircling an exceptional point for asymmetric mode switching. Nature **537**(7618), 76–79 (2016)
13. El-Ganainy, R., Makris, K.G., Christodoulides, D.N., Musslimani, Z.H.: Theory of coupled optical PT-symmetric structures. Opt. Lett. **32**(17), 2632–2634 (2007)
14. El-Ganainy, R., Makris, K.G., Khajavikhan, M., Musslimani, Z.H., Rotter, S., Christodoulides, D.N.: Non-Hermitian physics and PT symmetry. Nat. Phys. **14**(1), 11 (2018)
15. Ge, L., Türeci, H.E.: Antisymmetric PT-photonic structures with balanced positive-and negative-index materials. Phys. Rev. A **88**(5), 053810 (2013)
16. Gilary, I., Moiseyev, N.: Asymmetric effect of slowly varying chirped laser pulses on the adiabatic state exchange of a molecule. J. Phys. B **45**(5), 051002 (2012)

17. Gilary, I., Mailybaev, A.A., Moiseyev, N.: Time-asymmetric quantum-state-exchange mechanism. Phys. Rev. A **88**(1), 010102 (2013)
18. Goldzak, T., Mailybaev, A.A., Moiseyev, N.: Light stops at exceptional points. Phys. Rev. Lett. **120**, 013901 (2018)
19. Hau, L.V., Harris, S.E., Dutton, Z., Behroozi, C.H.: Light speed reduction to 17 metres per second in an ultracold atomic gas. Nature **397**(6720), 594–598 (1999)
20. Jackson, J.D.: Classical Electrodynamics. Wiley, Chichester (1999)
21. Klaiman, S., Günther, U., Moiseyev, N.: Visualization of branch points in PT-symmetric waveguides. Phys. Rev. Lett. **101**(8), 080402 (2008)
22. Kottos, T.: Optical physics: broken symmetry makes light work. Nat. Phys. **6**(3), 166–167 (2010)
23. Landau, L.D., Lifshitz, E.M.: Quantum Mechanics, Non-relativistic Theory. Pergamon, Oxford (1991)
24. Mailybaev, A.A.: Computation of multiple eigenvalues and generalized eigenvectors for matrices dependent on parameters. Numer. Linear Algebra Appl. **13**(5), 419–436 (2006)
25. Moiseyev, N.: Non-Hermitian Quantum Mechanics. Cambridge University Press, Cambridge/New York (2011)
26. Moiseyev, N., Friedland, S.: Association of resonance states with the incomplete spectrum of finite complex-scaled Hamiltonian matrices. Phys. Rev. A **22**(2), 618–624 (1980)
27. Mostafazadeh, A.: Pseudo-Hermiticity versus PT symmetry: the necessary condition for the reality of the spectrum of a non-Hermitian Hamiltonian. J. Math. Phys. **43**(1), 205–214 (2002)
28. Mostafazadeh, A.: Quantum brachistochrone problem and the geometry of the state space in pseudo-Hermitian quantum mechanics. Phys. Rev. Lett. **99**(13), 130502 (2007)
29. Peng, P., Cao, W., Shen, C., Qu, W., Wen, J., Jiang, L., Xiao, Y.: Anti-parity-time symmetry with flying atoms. Nat. Phys. **12**(12), 1139–1145 (2016)
30. Ruschhaupt, A., Delgado, F., Muga, J.G.: Physical realization of-symmetric potential scattering in a planar slab waveguide. J. Phys. A **38**(9), L171–L176 (2005)
31. Rüter, C.E., Makris, K.G., El-Ganainy, R., Christodoulides, D.N., Segev, M., Kip, D.: Observation of parity–time symmetry in optics. Nat. Phys. **6**(3), 192–195 (2010)
32. Schomerus, H., Wiersig, J.: Non-Hermitian-transport effects in coupled-resonator optical waveguides. Phys. Rev. A **90**(5), 053819 (2014)
33. Seyranian, A.P., Mailybaev, A.A.: Multiparameter stability theory with mechanical applications. World Scientific, Singapore (2003)
34. Seyranian, A.P., Kirillov, O.N., Mailybaev, A.A.: Coupling of eigenvalues of complex matrices at diabolic and exceptional points. J. Phys. A **38**(8), 1723–1740 (2005)
35. Siegman, A.E.: Propagating modes in gain-guided optical fibers. J. Opt. Soc. Am. A **20**(8), 1617–1628 (2003)
36. Tanaka, Y., Upham, J., Nagashima, T., Sugiya, T., Asano, T., Noda, S.: Dynamic control of the Q factor in a photonic crystal nanocavity. Nat. Mater. **6**(11), 862–865 (2007)
37. Uzdin, R., Mailybaev, A.A., Moiseyev, N.: On the observability and asymmetry of adiabatic state flips generated by exceptional points. J. Phys. A **44**(43), 435302 (2011)
38. Wang, L.J., Kuzmich, A., Dogariu, A.: Gain-assisted superluminal light propagation. Nature **406**(6793), 277–279 (2000)
39. Weiner, A.: Ultrafast Optics. Wiley, New York (2011)
40. Wigner, E.: On a modification of the Rayleigh–Schrdinger perturbation theory. Math. Natur. Anz. (Budapest) **53**, 477–482 (1935)
41. Withayachumnankul, W., Fischer, B.M., Ferguson, B., Davis, B.R., Abbott, D.: A systemized view of superluminal wave propagation. Proc. IEEE **98**(10), 1775–1786 (2010)
42. Wu, J.H., Artoni, M., La Rocca, G.C.: Parity-time-antisymmetric atomic lattices without gain. Phys. Rev. A **91**(3), 033811 (2015)
43. Xu, H., Mason, D., Jiang, L., Harris, J.G.E.: Topological energy transfer in an optomechanical system with exceptional points. Nature **537**(7618), 80–83 (2016)
44. Yanik, M.F., Suh, W., Wang, Z., Fan, S.: Stopping light in a waveguide with an all-optical analog of electromagnetically induced transparency. Phys. Rev. Lett. **93**(23), 233903 (2004)